Hysteresis in Stability Conditions of Electron-Hole Plasma

BETSY ANCKER-JOHNSON
Boeing Scientific Research Laboratories, Seattle, Washington
(Received 13 January 1964)

The investigation of the hysteresis occurring in the threshold conditions for the helical instability oscillations in electron-hole plasma has been extended. The hysteresis in electric field strength E can exceed 45 V/cm and 50% of the applied E at threshold. By determining the stability-instability boundary in the p-type InSb as a function of the parallel (or antiparallel) electric and magnetic field strengths and also the plasma density, the magnetic field induced by the formation of the helical density perturbation is deduced. Resulting displaced loop B-H curves are presented. The magnitude of the induction enhancement B_{hys} can be as large as 165 Oe and 55% of the applied B at threshold. The extent of applied magnetic field (or electric field strength) over which the loops can occur is limited at the high magnetic field end (typically ≤ 600 G) by vanishingly small plasma density and at the other end (≥ 280 G) by the occurrence of magnetic pinching. The loops are largest at the low magnetic field end. The range of loop energy, defined as the product of E_{hys} and B_{hys}, increases with decreasing plasma cross-sectional area until saturation occurs at a plasma radius of $\sim 3\times10^{-2}$ cm. The full range from largest to smallest loop in any one sample is achieved by a relatively small variation in the "input energies," i.e., the product of the magnetic and electric field strengths at threshold.

I. INTRODUCTION

IT is well known that the stability of a plasma may be enhanced by the application of a longitudinal magnetic field.[1] Early stability and confinement experiments also showed the existence of a definite limit to the improvement so obtainable. Indeed, too large a magnetic field causes the onset of oscillations in the plasma and its rapid radial diffusion to the container boundaries. The helical instability theory first proposed by Kadomtsev and Nedospasov[2] accounts for these occurrences and describes the boundary between stability and instability in terms of the applied, parallel electric and magnetic field strengths. Johnson and Jerde[3] supplied a firm mathematical base for the theory and improved its predictions.

Almost concurrently with these electron-ion plasma experiments,[1] Ivanov and Ryvkin[4] reported the occurrence of current oscillations in germanium immersed in a longitudinal magnetic field. Larrabee and Steele[5] made a detailed study of this phenomenon and named it the oscillistor. They demonstrated that the oscillations occur only if excess carriers, i.e., an electron-hole plasma, is present in the semiconductor. Glicksman[6] recognized the applicability of Kadomtsev and Nedospasov's theory to this phenomenon and adapted it to electron-hole plasmas in an insulator. Holter[7] used Johnson and Jerde's[3] approach to derive again explicit expressions for the threshold frequency and electric field strength as functions of magnetic field strength, some parameters of the plasma and its container (the semiconductor), this time applicable also to both extrinsic and intrinsic semiconductors as well as to insulators. His comparison with Ancker-Johnson's[8] measurements of the threshold conditions showed good agreement. Other data[9,10] on the threshold conditions which do not include the densities of the plasmas, a parameter of the theory, are compatible with theory.

Recently, hysteresis in the conditions necessary for the production of the helical instability oscillations in electron-hole plasmas was reported along with the suggestion of its practical application to memory devices.[11] This hysteresis differs from the familiar type possessed, for example, by ferrites, in that it exhibits two loops which are displaced from the origin of the B–H curve, as illustrated by Fig. 1(a). A plasma is

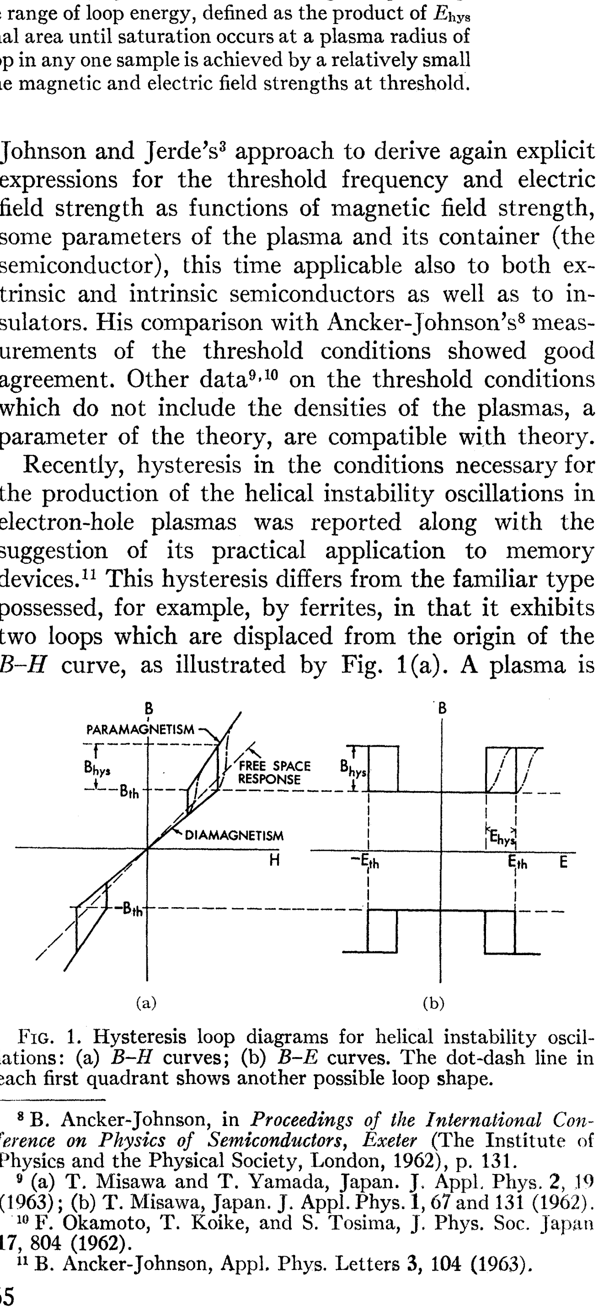

FIG. 1. Hysteresis loop diagrams for helical instability oscillations: (a) B–H curves; (b) B–E curves. The dot-dash line in each first quadrant shows another possible loop shape.

[1] B. Lehnert, in *Proceedings of the Second United Nations International Conference on Peaceful Uses of Atomic Energy, Geneva* (United Nations, Geneva, 1958), p. 146.
[2] B. B. Kadomtsev and A. V. Nedospasov, J. Nucl. Energy **1**, 230 (1960); see F. C. Hoh, Rev. Mod. Phys. **34**, 267 (1962) for a review of experiments and theories of the helical instability in electron-ion plasmas.
[3] R. R. Johnson and D. A. Jerde, Phys. Fluids **5**, 988 (1962).
[4] I. L. Ivanov and S. M. Ryvkin, Zh. Techn. Fiz. **28**, 774 (1958) [English transl: Soviet Phys.—Tech. Phys. **3**, 722 (1958)].
[5] R. D. Larrabee and M. C. Steele, J. Appl. Phys. **31**, 1519 (1960); R. D. Larrabee, J. Appl. Phys. **34**, 880 (1963); see also, J. Bok and R. Veilex, Compt. Rend. **248**, 2300 (1958).
[6] M. Glicksman, Phys. Rev. **124**, 1655 (1961).
[7] O. Holter, Phys. Rev. **129**, 2548 (1963); for more details see Boeing Scientific Research Labs Document D1-82-0198, September 1962 (unpublished), or Årbok Univ. i Bergen, Mat.-Nat., Ser. **8**, 3 (1963).
[8] B. Ancker-Johnson, in *Proceedings of the International Conference on Physics of Semiconductors, Exeter* (The Institute of Physics and the Physical Society, London, 1962), p. 131.
[9] (a) T. Misawa and T. Yamada, Japan. J. Appl. Phys. **2**, 19 (1963); (b) T. Misawa, Japan. J. Appl. Phys. **1**, 67 and 131 (1962).
[10] F. Okamoto, T. Koike, and S. Tosima, J. Phys. Soc. Japan **17**, 804 (1962).
[11] B. Ancker-Johnson, Appl. Phys. Letters **3**, 104 (1963).

TABLE I. Sample properties and hysteresis data. See Fig. 3 for dimensions.

Sample No.	Initial hole density (cm^{-3})	Hole mobility (cm^2/V-sec)	E_{th}(V/cm)	B_{th}(G)	ξ	E_{hys}(V/cm)	B_{hys} deduced from Experimental ξ boundary	Constant ξ boundary
2D-2	4.9×10^{14}	8600	99.5	282	0.53[a]	35	65	20
			86.5	302.5	0.24[a]	26	65	18
			75	317	0.15[a]	17	62	13
			69	337	0.08_5	13	48	9
			63.5	355	0.04_5	10	48	8
			56.5	385	0.02_3	9	59	7
			51.5	417	0.01_2	6	38	6
2D2-7	5.0×10^{14}	8300	89.5	299	0.12_2[a]	48.5	165.5	61
			74	325	0.07_4[a]	34	144	68
			66	365	0.05_6	29	114	47
			63	376	0.04_9	21	83	36
			60.5	390	0.04_2	14.5	54	20
			52	421	0.02_8	10	38	11
2D2-8	4.3×10^{14}	7200	164	345	0.08_7	40	93	31
			159	370	0.07_8	42	91	26
			143	394	0.05_8	32	88	18
			127	430	0.03_2	24	80	26
			118	460	0.03_1	19	64	21
			110	485	0.02_2	14.5	51	15
			103	510	0.01_8	9.5	34	6
2D2-2	3.7×10^{14}	7000	85.5	390	0.11_3	22.5	69	37
			79	410	0.10_0	18	59	28
			73	430	0.08_5	15	55.5	24
			66	450	0.07_2	13	59.5	...
			60	471	0.06_1	11.5	70.5	27
			57	490	0.05_5	10.5	77	...
			53	510	0.04_8	9	82	30
			50	530	0.04_2	8	87	30
			48	550	0.03_9	7	80	28
			46	570	0.03_3	6	70	24
			44.5	590	0.03_2	5	53	20
			42.5	610	0.02_7	3	36	12

[a] Obtained by extrapolation of the I–V characteristic after the onset of current pinching.

normally diamagnetic but at the onset of the helical instability it becomes paramagnetic as experimentally demonstrated in an electron-ion plasma by Johnson.[12] This paramagnetism occurs because the formation of the helical density perturbation produces an enhanced induction. The hysteresis follows from the fact that as the applied magnetic field is reduced, the threshold induction is not reached until the applied field has a smaller magnitude than it had at the onset of instability. Drummond[13] first deduced that Johnson's results implied the existence of such a new hysteresis effect. The hysteresis observed[11] in an electron-hole plasma is an hysteresis in the parameter which defines the boundary between a stable and unstable plasma, namely the magnitude of the produce of the electric and magnetic fields, as illustrated in Fig. 1(b). The present paper extends these hysteresis measurements to the determination of the induction enhancement caused by the helical instability and, hence, B–H curves of the type illustrated in Fig. 1(a) are presented.

[12] R. R. Johnson, in *Proceedings of the Sixth International Conference on Ionization Phenomena in Gases* (Paris, 1963), Vol. I, p. 413.

[13] J. E. Drummond, Boeing Scientific Research Laboratories Progress Review, First Six Months 1963 (unpublished), p. 95.

II. EXPERIMENT

The circuit is the same as that employed previously.[11] It consists simply of a triangular waveform delivered to a single crystal parallelepiped of p-type InSb at 77°K in the presence of a magnetic field which is applied essentially parallel to the direction of current flow. The plasma is produced by injection[14] from indium solder contacts of various cross-sectional area. The electric field strength is determined by measuring the potential difference between two very small contacts spaced a known distance apart. The series of measurements reported here involves four samples of similar bulk properties but different dimensions and contact arrangements as recorded in Table I. The waveform of the

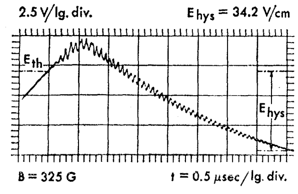

FIG. 2. An oscillogram showing hysteresis in the threshold electric field strength while the plasma is immersed in a constant magnetic field intensity.

[14] B. Ancker-Johnson, R. W. Cohen, and M. Glicksman, Phys. Rev. **124**, 1745 (1961).

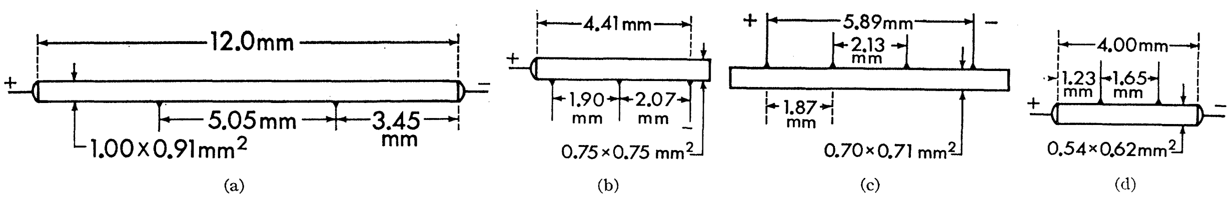

FIG. 3. Dimensions of samples. (a) 2D-2, (b) 2D2-7, (c) 2D2-8, (d) 2D2-2.

helical instability oscillations is markedly affected by the degree of parallelism (as also noted previously[5]) between the applied magnetic field and the direction of current flow, particularly in the cases of nonsymmetric current contacts (samples 2D2-7 and 2D2-8). By careful adjustment it was always possible to obtain essentially sinusoidal oscillations as illustrated by Fig. 3(d) of Ref. 11.[15]

The use of a triangular input waveform enables the simultaneous determination of the following pertinent parameters: the electric field strength threshold E_{th} at a given magnetic field strength B_{th}, and the difference in electric field strength at the onset and cessation of oscillations E_{hys}, as Fig. 2 illustrates. A separate measurement of the current-voltage characteristics (see Figs. 1 and 4 of Ref. 8 and Fig. 5 of Ref. 14, for examples) relates E_{th} to the total current and, by subtraction of the extrapolated Ohmic current, to the plasma current. Hence the boundary between stability and instability may be delineated by plotting B_{th} as a function of E_{th} with the ratio of the injected plasma density to the initial density of carriers (or background plasma density) ξ as a parameter. (See Part IV for method of calculating ξ.)

Two examples of boundary diagrams are shown in Figs. 4 and 5. The correpsonding ξ parameters for each measured point on the boundary are listed in Table I. As the electric field strength is increased with the plasma immersed in a constant magnetic field, oscillations commence at the conditions corresponding to the circles. A line connecting these points defines the boundary, a line which has no characteristic locus since the third controlling parameter ξ is arbitrarily fixed by the injection properties of the particular contacts. In practice, however, each boundary is of such a shape that the product of the threshold electric and magnetic fields is very approximately a constant. The conditions marked by the triangles on Figs. 4 and 5 indicate the observed hysteresis in electric field strength, i.e., the lower than E_{th} values at which oscillations are observed to cease.

A square-wave input was also employed whose rise and fall times (<13 nsec) are less than the period of these helical instability oscillations. With a circuit identical to that in which the triangular-waveform input is used, except for the absence of the capacitance to ground which makes the square-wave triangular, oscillations do not persist after cutoff of the square wave from an electric field strength greater than E_{th} to one less than that at which oscillations cease when a slowly falling E is applied, i.e., $E<(E_{\mathrm{th}}-E_{\mathrm{hys}})$. Thus, E_{hys} cannot be attributed to a slowly damping oscillation.

E_{th} is constant to within $\pm 5\%$ when the magnitude of the peak value of the applied field strength is varied from E_{th} to $2E_{\mathrm{th}}$. The magnitude of the field strength at which the oscillations cease is constant to within $\pm 3\%$ for the same excursion into the supercritical region and, in fact, deviations can only be observed when the maximum field strengths are close to E_{th}. Variations in the time-rate-of-change of the applied field strength by as much as a factor of 4 also do not affect E_{th} and E_{hys} beyond the above-stated limits.

By completing the loops as drawn in Figs. 4 and 5 the enhancement in the magnetic induction caused by the formation of the helical instability may be deduced. The influence of the parameter ξ in deducing this enhancement is discussed in Sec. IV. Figure 4 records more typical results than Fig. 5 which shows the occurrence of some very large induction enhancements.

The larger magnitudes of the hysteresis electric field strengths, E_{hys} and larger induction increases, B_{hys},

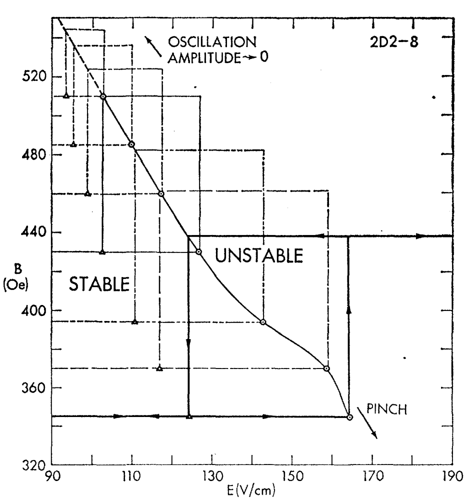

FIG. 4. A typical B–E threshold diagram showing the boundary between a quiescent and a rotating plasma. The circles which define this boundary correspond to the measured E_{th} at the onset of oscillations and the triangles indicate the measured electric field strengths at cessation, $(E_{\mathrm{th}}-E_{\mathrm{hys}})$. Simplified hysteresis loops corresponding to these thresholds are drawn.

[15] Small deviations (e.g., ~1°) from the alignment between the direction of current flow and the magnetic field yielding the most nearly sinusoidal oscillations do not noticeably affect E_{th} and E_{hys}.

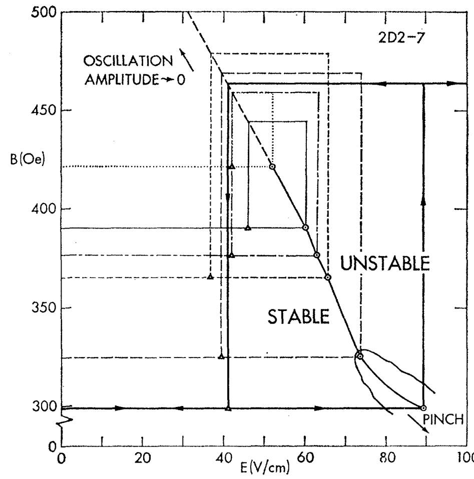

FIG. 5. A B–E threshold diagram exhibiting very large hysteresis loops.

and, therefore, the larger hysteresis loops, accompany the smaller applied magnetic fields as Figs. 4 and 5 and Table I show. The E_{hys} decreases steadily with increasing applied magnetic field but the magnitude of B_{hys} (Table I) depends on the shape of the instability boundary. If the boundary is steep at the high B end, i.e., $|dB/dE|$ is large, the B_{hys} values do not steadily decrease with increasing applied magnetic field, as in the case of samples 2D-2 and 2D2-2 whose $|dB/dE|$ at the high B end of the instability boundary are 6.5 and 7.0, respectively, compared with 3.8 and 4.2 for 2D2-8 and 2D2-7. Independent of $|dB/dE|$, however, is the fact that the hysteresis magnetic fields are smallest at the highest applied magnetic fields.

The extent of the B–E boundary over which hysteresis loops can occur is limited by two factors: At high electric field strengths and, therefore, high currents, the magnetic (Bennett) pinch effect[8,14] prevails which inhibits the helical instability. Oscillations may still occur when the pinch is well formed but these pinch-unpinch[8] and magnetothermal[16] oscillations are very different and easily distinguished from helical instability oscillations.[17] As indicated by the wavy line in Fig. 5, pinching begins in this sample at ~73 V/cm so the high electric field strength extreme of this boundary is somewhat affected by weak pinching. A detailed comparison with theory (see next section) shows that the onset of pinching tends to make the measured threshold deviate from the actual boundary toward higher E_{th}. At the other extreme of the hysteresis range, namely at the low electric field strengths, the plasma density becomes vanishingly small along with the amplitude of oscillations and the hysteresis effect. The ratio of plasma-to-background-density ξ at the lowest electric field strengths for which hysteresis can be readily observed range typically from 1 to 3% (cf. Table I).

Measuring directly the magnitudes of the magnetic fields produced by the helical paths of plasma current is difficult, principally because of the relatively small sample sizes and large currents. Inadequate electrostatic shielding plus the unavailability of a sufficiently high current source which could be appropriately modulated prevents the use of pickup coils, a highly satisfactory method for such magnetic field measurements in electron-ion plasmas.[12] Hall probes, however,

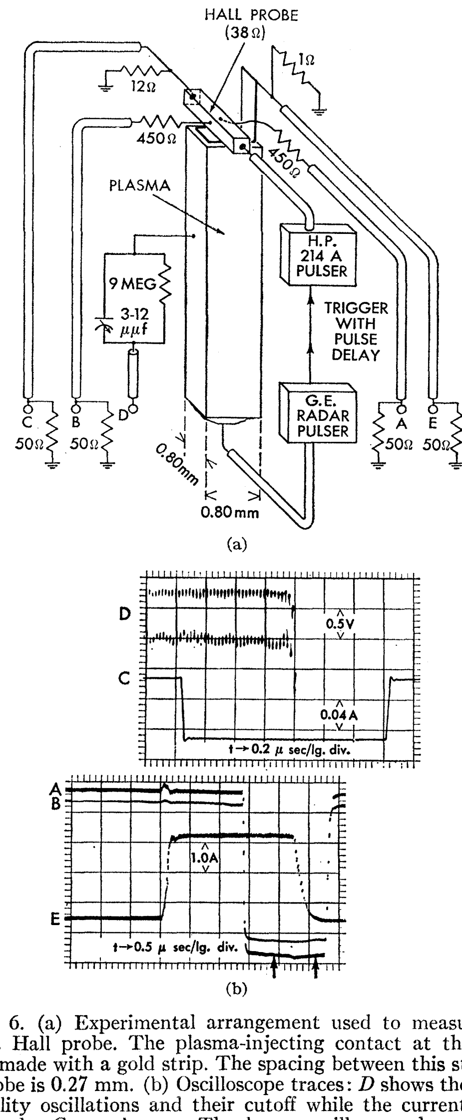

FIG. 6. (a) Experimental arrangement used to measure B_{hys} with a Hall probe. The plasma-injecting contact at the probe end is made with a gold strip. The spacing between this strip and the probe is 0.27 mm. (b) Oscilloscope traces: D shows the helical instability oscillations and their cutoff while the current in the Hall probe C remains on. The lower oscillogram has a faster sweep time and shows both the beginning and end of the current pulse in the plasma E. Traces A and B correspond to the voltages on the Hall probe side contacts.

---

[16] B. Ancker-Johnson, Phys. Rev. Letters **9**, 485 (1962); J. E. Drummond and B. Ancker-Johnson, Bull. Am. Phys. Soc. **8**, 471 (1963); **9**, 318 (1964).

[17] M. C. Steele and T. Hattori [J. Phys. Soc. Japan **17**, 1661 (1962)] offer an explanation of some very small amplitude oscillations observed during pinching by M. Glicksman and R. A. Powlus [Phys. Rev. **121**, 1659 (1961)] in impact-ionization plasmas in n-type InSb which is related to the generation of sound waves. Impact ionization is not occurring in the present experiments.

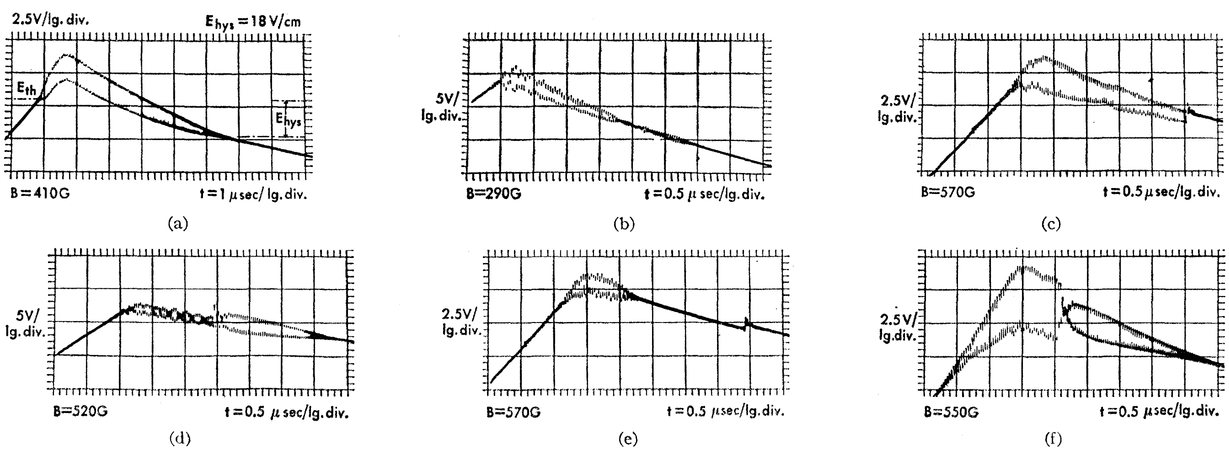

FIG. 7. Oscilloscope diagrams illustrating some of the startling properties of the oscillatory behavior.

do yield a direct estimate when the arrangement shown in Fig. 6 is employed. A small parallelepiped of n-type InSb is located orthogonally to a plasma-containing sample, so that the former senses the applied longitudinal magnetic field as well as the helix field, but not azimuthal fields produced by current flow.

The Hall probe circuit is supplied with resistances such that the transmission line is everywhere matched and the voltage contacts A and B are effectively isolated from the current path. The outputs of A and B are fed into a storage oscilloscope (Tektronics No. 564) equipped with a sampling dual-trace plug-in unit (No. 3S76). These voltages, at a time selected with the manual scan of a sampling sweep plug-in unit (No. 3T77) and indicated by the arrows at the bottom of Fig. 6(b), are taken from the output jacks of the dual-trace unit through two bucking voltages supplies and a pair of dc amplifiers. The difference between these signals is then read on a voltmeter which is directly calibrated in gauss by varying the applied longitudinal magnetic field. The bucking voltages are adjusted to maximize the sensitivity: No signal is detected when the applied magnetic field is on but no oscillations are present [right-hand arrow in Fig. 6(b)], so that only the field added by the helix is measured when the manual scan is located at the left-hand arrow. Although the sensitivity of this system is ~ 1 G, drifting of the zero makes the measurements tedious. The results are summarized in Table II.

Certain observed aspects of the hysteresis effect are quite startling. Some are illustrated by the oscillograms of Fig. 7. The first, 7(a), shows how rapidly the amplitude of oscillations can grow to surprisingly large amplitudes in an otherwise perfectly typical hysteresis oscillogram. Oscillations can apparently cease as the electric field strength decreases to some magnitude and then with further decrease commence again, 7(b).[18] Unusually large amplitude oscillations occasionally cease suddenly with decreasing electric field strength, producing a discontinuity in the average E, 7(c). A sudden switch from moderate to larger amplitude oscillations can also occur during decreasing E, 7(d). No hysteresis or a "reverse hysteresis," an anomaly in itself, can be followed by a sudden discontinuity in the measured E at some E well below $(E_{\text{th}}-E_{\text{hys}})$, 7(e). Rare but reproducible is the oscillatory pattern displayed in 7(f). The input waveform was monitored before each of these oscillograms was made and found to be smooth as usual.

Detailed observations regarding threshold frequency (i.e., frequency at the instability boundary) cannot be made from this type of data since the frequency is a function of electric field strength in the supercritical region.[2,3,6–10]

III. THEORY

The helical instability[2,3,6,7] is a growing helical density perturbation superimposed on an unperturbed, steady-state plasma density and electric potential in a plasma column immersed in parallel (or antiparallel) electric and magnetic fields.[19] The perturbed density and potential are assumed to have the following forms, respectively,

$$n_i = n_{i,0} + f(r,z)\exp[ikz+im\theta+i\omega t], \tag{1}$$

$$U = U_0 + g(r)\exp(ikz+im\theta+i\omega t], \tag{2}$$

TABLE II. Hall probe measurements on sample 2D2-13.

Bulk properties	$B_{\parallel}(G)$	$I_p(A)$	when $B_{\text{helix}}(G)$ at end is:	$I_p(A)$ at threshold
$p_0 = 3.5\times10^{14}$ cm^{-3}	340	1.9	10 ± 2	0.4
$\mu_p = 8000$ cm^2/V-sec	320	2.3	13 ± 2	0.5

[18] A possibly related and also as yet not understood effect was noted in Ref. 8: As the magnetic field strength was increased above threshold while the total current was held constant, the oscillations became noisy and then another "mode" at a higher frequency emerged before noise ultimately resulted.

[19] F. C. Hoh and B. Lehnert, Phys. Rev. Letters 7, 75 (1961) give one simple, physical interpretation of the theory.

where f and g are small quantities compared with $n_{i,0}$, the steady-state density and U_0, the steady-state potential, respectively. The quantity k is the wave number along the z axis, m is the wave number in the azimutual direction ($m=1$ for helix) and ω is the frequency of the perturbation.

The plasma is assumed to be collision dominated. It is described by the continuity equations

$$(\partial n_{i\pm}/\partial t)\pm\nabla\cdot\{(n_{0\pm}+n_{i\pm})v_{\pm}\}=\gamma n_{i\pm}, \tag{3}$$

and the equations of motion

$$\begin{aligned}D_{\pm}\nabla n_{i\pm}=&\pm(\mu_{\pm}/c)(n_{0\pm}+n_{i\pm})\mathbf{v}_{\pm}\times\mathbf{B}\\&\pm\mu_{\pm}(n_{0\pm}+n_{i\pm})\mathbf{E}-(n_{0\pm}+n_{i\pm})\mathbf{v}_{\pm}\\&-(\partial/\partial t)[(n_{0\pm}+n_{i\pm})\mathbf{v}_{\pm}]\nu_{\pm}^{-1}.\end{aligned} \tag{4}$$

The last term in (4) is negligible because the collision frequencies $\nu_{\pm}$ are so large. The subscripts $\pm$ refer to holes and electrons, respectively; γ is the recombination and generation coefficient; n_0 is the density of initial carriers, D is the diffusion constant, μ the mobility and v the velocity. An essentially neutral injected plasma $|n_{i+}-n_{i-}|\ll|n_{i\pm}|$ with equal electron and hole temperatures is assumed. Even at relatively elevated electric field strengths ($\sim$200 V/cm) equal temperatures seems to be the most reasonable assumption.[20]

A dispersion relation for the frequency is derived from Eqs. (1) and (2) and the boundary between stability and instability occurs when $\mathrm{Im}(\omega)=0$. Using the additional condition[3,7] that the derivatives of Im (ω) with respect to k must equal 0 at the onset of instability, the electric field strength (also the wavelength and frequency of oscillation) is expressed in terms of the threshold magnetic field strength.

Holter[7] has taken into account that the flow of current causes plasma heating above the semiconductor lattice temperature, here $V_0=6.6\times10^{-3}$ eV. Hence the mobilities are expressed as

$$\mu_{\pm}=\mu_{0\pm}(V_0/V)^{\alpha}, \tag{5}$$

where $\mu_{0\pm}$ are the hole and electron mobilities, respectively, at V_0 which is less than the plasma temperature V. For InSb in the temperature range of interest $\alpha\approx0.5$. Then dimensionless threshold magnetic and electric field parameters may be expressed, respectively, as

$$y=y_0(V_0/V) \tag{6}$$

and

$$\mathcal{E}=\mathcal{E}_0(y/y_0). \tag{7}$$

With the use of these definitions

$$y_0=\mu_{0-}\mu_{0+}B_{\mathrm{th}}^2, \tag{8}$$

$$\mathcal{E}_0=E_{\mathrm{th}}R/V_0. \tag{9}$$

R is the radius of the plasma. Equation (7) is obtained by eliminating the temperature V when Eqs. (6) and (9) are combined. In the limit of small threshold magnetic fields, i.e., $y\ll1$, which is the case in these experiments, $\mathcal{E}$ has an asymptotic solution which may be expressed as

$$\mathcal{E}=K_0y^{-1/2}. \tag{10}$$

K_0 is dependent on the injected-plasma-to-background-density ratio ξ but not on magnetic field, hence, it may be evaluated for a particular $y\ll1$, e.g., $y_1=10^{-3}$. Then the corresponding values of $\mathcal{E}_1$ are known as a function of ξ and the plasma temperature is found by equating Eqs. (7) and (6) and using (9) and (10):

$$V=\left[\frac{y_0V_0}{y_1}\left(\frac{E_{\mathrm{th}}R}{\mathcal{E}_1}\right)^2\right]^{1/3}. \tag{11}$$

A nonlinear theory treating the hysteresis effect itself in electron-ion plasmas has been worked out by Holter and Johnson.[21] Such a theory applicable to electron-hole plasmas is as yet lacking.

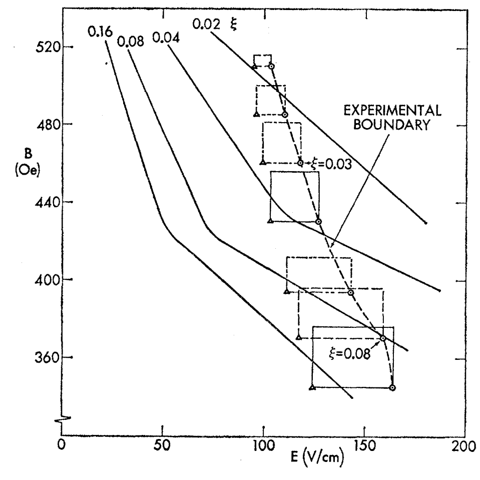

FIG. 8. B–E threshold diagrams for plasmas of constant densities in the same sample as used to obtain the data in Fig. 4. Simplified hysteresis loops corresponding to constant ξ values are shown. The experimentally determined threshold boundary (nonconstant ξ) is also indicated. The ξ values for two experimental points are identified for an illustration (see text).

IV. DISCUSSION

The parameter ξ is estimated from the readily obtainable Ohmic and total current magnitudes, respectively,

$$I_{\Omega}=ep_0\mu_{0+}EA, \tag{12}$$

$$I_T=I_{\Omega}[1+((\mu_{0-}/\mu_{0+})+1)n/p_0], \tag{13}$$

as

$$\xi\approx\frac{n}{p_0}=\frac{I_T-I_{\Omega}}{I_{\Omega}((\mu_{0-}/\mu_{0+})+1)}, \tag{14}$$

when A is the cross-sectional area of a semiconductor

[20] M. Glicksman and W. A. Hicinbothem, Jr., Phys. Rev. **129**, 1572 (1963).

[21] O. Holter and R. R. Johnson, Boeing Document D1-82-0256, December 1963 (unpublished).

containing an intial density of holes p_0 and a plasma of density n. The experimental ξ values are listed in Table I. (The radius of the plasma assumed for the calculations is that of the inscribed circle within each semiconductor cross section.) The calculated temperatures of the plasmas at the instability threshold ranged from 5.9×10^{-2} to 1.1×10^{-2} eV while the lattice remains at the bath temperature.

The influences of ξ on the enhancement in B caused by the presence of an helical current path are considered in the following: As E increases so does the plasma density which is injected by the current contacts, and as E exceeds E_{th} more and more of the plasma current goes into a helical path producing an enhanced B. When E decreases, the total $B=B_{\mathrm{applied}}+B_{\mathrm{helix}}$ remains greater than B_{th} even though the plasma current I_p is decreasing. Thus, a cessation of oscillation occurs at an $I_p<I_p$ at threshold and, therefore, at a ξ value $<\xi_{\mathrm{th}}$. This fact and its influence on the magnitude of the deduced B_{hys} is illustrated by Figs. 8 and 9. The lines labeled with numbers represent the threshold conditions for constant ξ values. The experimental threshold points are represented by circles and the triangles refer to conditions at cessation of the oscillations, consistent with the symbols in Figs. 4 and 5. At both threshold and cessation the amplitude of the oscillations is vanishingly small (cf. Fig. 2) and, hence, the perturbation theory[7] is applicable.

Hysteresis loops are drawn in Figs. 8 and 9 corresponding to constant ξ-value boundaries. The resulting B_{hys} are smaller than those deduced for nonconstant ξ boundaries, Table I. In general, the magnitude of I_p at some operating point in the supercritical region determines the B produced by the helix. If ξ were made independent of E and constant, e.g., by supplying the plasma optically when noninjecting contacts carry the current, the smaller set of B_{hys} magnitudes would

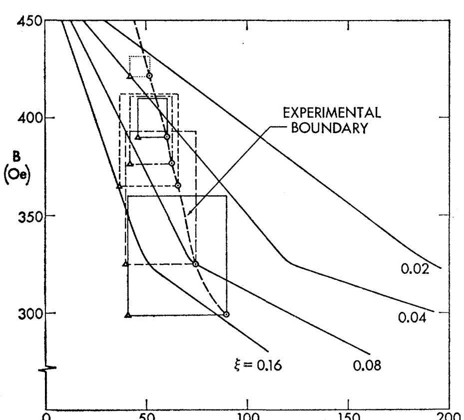

FIG. 9. B–E threshold diagrams for plasmas of constant density in the same sample as used to obtain the data in Fig. 5. Simplified hysteresis loops corresponding to ξ values are shown. The experimentally determined threshold boundary (nonconstant ξ) is also indicated.

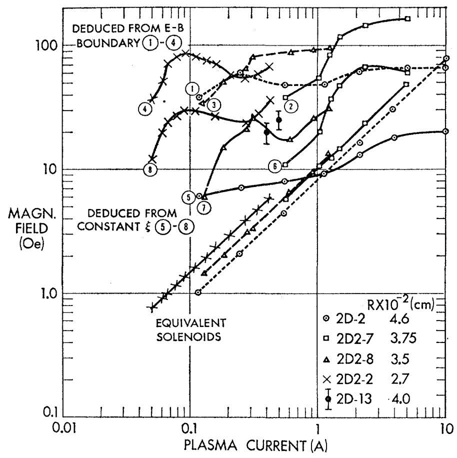

FIG. 10. Magnetic field is plotted as a function of plasma current using: (1–4) the experimentally deduced B_{hys} values (nonconstant ξ); (5–8) B_{hys} values derived from constant ξ conditions; and calculated B values produced by solenoids of equivalent turns ratio. The two points with error brackets represent the results of Hall probe measurements.

result. Conversely, the steeper the I–V characteristic and, therefore, the more rapid the increase of plasma density with E, the steeper the B–E boundary and the larger resulting B_{hys}. Sample 2D2-7 compared with 2D2-8 is an example of the latter case (Figs. 5 and 4).

Reference to a particular set of operating conditions (see Figs. 4 and 8) clarifies these statements: A threshold for the helical instability in sample 2D2-8 is at $B=370$ G, $E=159$ V/cm and $\xi=0.08$. The plasma becomes quiescent again at $E=E_{\mathrm{th}}-E_{\mathrm{hys}}=117$ V/cm and: (a) for a constant plasma density and therefore $\xi=0.08$ at $B=B_{\mathrm{th}}+B_{\mathrm{hys}}=370+26=396$ G; (b) for a plasma density dictated by the properties of the current injecting contacts $\xi=0.03$ at $B=370+91=461$ G.

The magnitude of the fields produced by the helices are plotted in Fig. 10 as a function of the plasma current at the threshold. Curves 1 through 4 refer to the experimentally determined threshold boundaries and 5 to 8 to boundaries of constant plasma density. The shape of each of these curves is controlled, as stated earlier in connection with Figs. 4 and 5, by the arbitrary properties of the injection contacts. The two points with error brackets represent the results of the Hall probe measurements. These two points are plotted at the threshold plasma current, consistent with the rest of the data points, although the measurements were made at higher currents, Table II. Also graphed in this figure are the magnetic fields that solenoids would produce which possess the same radius and number of turns per cm as the helical instability in the four samples. The turns ratios of the equivalent solenoids are derived from Holter's calculation of the wavelength of the helix at threshold (Fig. 1, Ref. 7). The dimensionless wavelength λ/R is nearly constant for all the present measurements; it varies only between 3.2 and 3.6. The radius R (Table I) has a range of less than a factor of 2, hence

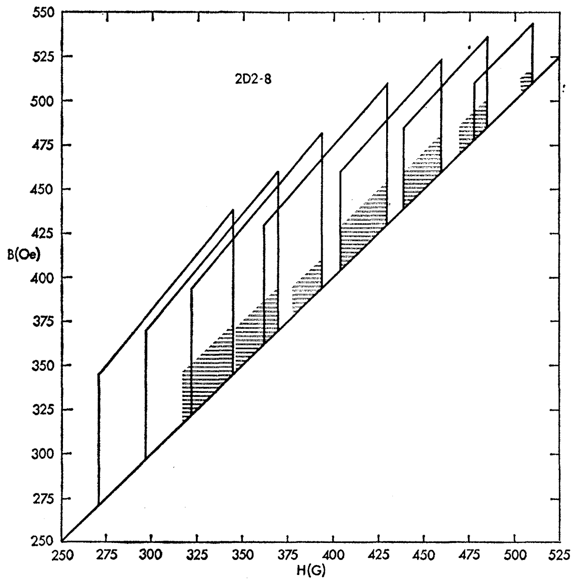

FIG. 11. The first quadrant of deduced B–H curves. The larger loops correspond to Fig. 4 and the smaller (hatched) to Fig. 8.

the fields produced by the equivalent solenoids are essentially determined by the magnitude of the current they carry. The equivalent solenoid results in Fig. 10 are obtained with the assumption that all the plasma current goes into the helix at threshold which, of course, is not compatible with the perturbation theory.

Figure 10 indicates that the equivalent solenoids produce far less B than their counterparts in the plasma at low I_p even though it was assumed that they carry all the plasma current. The fields deduced from the boundary measurements, however, result from excursions into the supercritical region, hence curves 1 to 8 should be shifted toward higher currents for comparison with the solenoid curves. The fields sensed by the Hall probes, when plotted against the I_p they carried during the measurements (Table II), agree well with the fields produced by equivalent solenoids conducting the same current. The agreement may be so good fortuitously since the λ of the helix in the supercritical region may not be constant in the range of these threshold magnetic fields. There is experimental evidence to suggest it is not constant[8,22] but a nonlinear theory for electron-hole plasmas, as stated earlier, is not available.

The Hall probe measurements were made on a sample with radius somwhat larger than 2D2–7. At $I_p=0.5$ A the B_{hys} deduced from the experimentally determined threshold boundary is $\sim$35 G whereas that deduced from the constant-plasma-density boundary is $\sim$10 G. Since the Hall-probe value of $\sim$26 G is likely to be too small because the measurements were made a finite distance from the end of the plasma helix [Fig. 6(a)], agreement with the experimentally determined B_{hys} value is indicated.

The magnitude of B_{hys} is very large compared with the part of it associated with the diamagnetism normally exhibited by a plasma. Recently Moore and Kessler[23] have measured the magnetic moment of an optically injected plasma in Ge. For a plasma density equal to 10^{15} cm^{-3} and an essentially infinite surface recombination velocity, a condition corresponding to the highest magnetic moment, they find a diamagnetic moment density of $\sim 2\times10^{-5}$ cgs units at 1 kG. The plasmas utilized in the present experiments can be expected to exhibit an even smaller moment since the plasma densities are 1 to $2\frac{1}{2}$ orders of magnitude smaller and the surface recombination velocity is finite. Hence essentially all of the deduced B_{hys} is associated with the paramagnetism produced by the helical instability. The first quadrant of the resulting B–H curves corresponding to Figs. 4 and 8 (the more typical set of hysteresis loops) is shown in Fig. 11. The larger loops correspond to the experimentally determined threshold boundary and the smaller loops (hatched) to the constant ξ boundary. The full B–H diagrams for sample 2D2-7, which exhibited the largest loops, are shown in Fig. 12. The loops are again drawn with straight sides for simplicity but their shapes cannot be ascertained by the present experiments.

The sign of the enhanced induction associated with the helical instability is positive as stated in the introduction, according to Johnson's measurements in electron-ion plasmas[12] and as verified by the described Hall probe measurements. This switch from diamagnetism to paramagnetism is completely compatible with

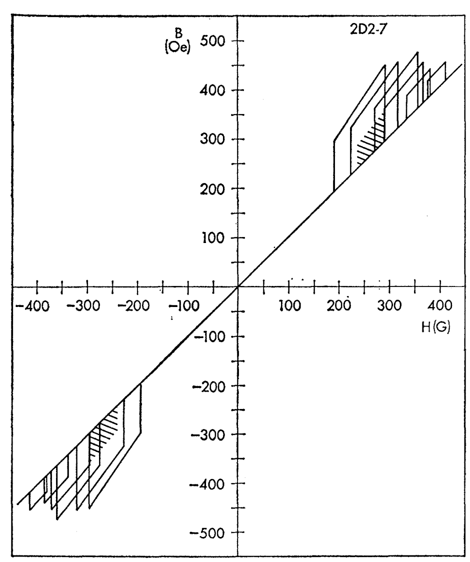

FIG. 12. Deduced B–H diagrams. The larger loops correspond to Fig. 5 and the smaller (hatched) to Fig. 9.

[22] The only published wavelength measurements known to the author are in Ref. 9. These results yield a λ/R 4 to 5 times Holter's calculated values. This makes the equivalent solenoid fields even smaller.

[23] A. R. Moore and J. O. Kessler, Phys. Rev. **132**, 1494 (1963). The author is grateful to Dr. Moore for discussing their results prior to publication.

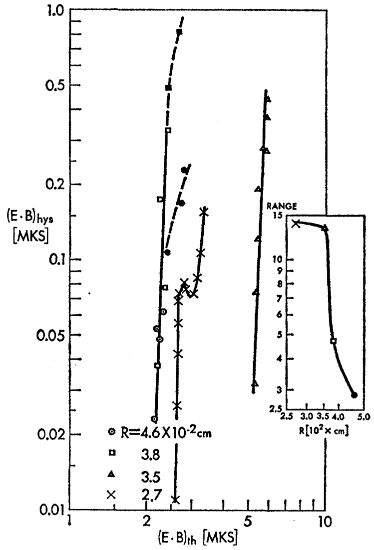

FIG. 13. The hysteresis loop energy as a function of the input energy at threshold for the experimentally determined boundaries, i.e., ξ nonconstant. The solid points represent hysteresis energy in a weakly pinched plasma. The insert shows the range of hysteresis loop energy as a function of plasma radius.

the helical instability theory[9b] which states that the the helical instability theory which states that the sense of the helix is positive (negative) with respect to the applied magnetic field when the applied E is parallel (antiparallel), and is independent of the drift direction of the helical density perturbation. Enhancement of the magnetic field results and, therefore, paramagnetism. That paramagnetism results is also evident from simple physical reasoning: Since the application of a B, large compared to B_{th}, causes a shift in the equilibrium position of the plasma toward its container walls, the magnetic pressure inside the helix must be greater than that outside, thus the magnetic field produced by the helix must *add* to the applied B.[24]

The effect of the plasma radius on the hysteresis is illustrated by Fig. 13 in which a measurement of the "hysteresis loop energy" is plotted against the "input energy" required to achieve oscillations for the four different plasma radii. The input energy necessary to produce hysteresis is quite constant as expected from both theory and the experimental results shown in Figs. 4 and 5. The theoretical curves of E_{th} as a function of B_{th}^2 have a slope of -0.5, hence for any one value of ξ the product $E_{\mathrm{th}}\times B_{\mathrm{th}}$ is a constant as illustrated by the hyperbolic boundaries for constant ξ values drawn in Figs. 8 and 9. Since ξ varies in the experiments (Table I), this product is only approximately constant. Of considerable practical interest is the fact that very little change in input energy is necessary for very large changes in loop energy. The greatest range in loop energy, defined as the ratio of the loop energy at the lowest $(E\times B)$ at which observable hysteresis occurs to the loop energy at the highest $(E\times B)$ at which noise-free oscillations occur, is produced by the smallest diameter plasma, if pinching is avoided. The insert in Fig. 13 indicates that the range saturates with decreasing plasma radius at $\sim 3\times 10^{-2}$ cm. If weak pinching is allowed, there appears to be an optimum intermediate plasma radius for obtaining the greatest hysteresis range.

The startling oscillatory behavior illustrated by Figs. 7(b)–(f) may be related to a complicated relationship between the direction of current flow and the applied magnetic field direction, since such behavior has not been observed in the two samples investigated which possess symmetrically located plasma injectors, namely samples 2D-2 and 2D2-2.

V. CONCLUSION

The hysteresis in electric field strength E accompanying the onset and cessation of the helical instability can exceed 45 V/cm and 50% of the applied E at threshold. The attendant hysteresis in magnetic field intensity B, deduced from measurements of the boundary conditions between a quiescent and a rotating plasma which agree well with theory, can exceed 160 G and 55% of the applied B at threshold. Hall probe measurements of the B produced by the helical path of plasma current tend to verify the deduced B_{hys} values both in magnitude and sign (paramagnetic). The resulting, novel B–H curves consist of loops which are displaced from the origin. An infinite number of hysteresis loops can be generated by a small variation in input energy $(E_{\mathrm{th}}\times B_{\mathrm{th}})$. The extent in E (or B) over which loops can occur is limited at the high E (low B) end by the onset of current pinching and at the low E (high B) end by vanishing plasma current and, hence, vanishing hysteresis. The existence of the largest loops at low magnetic fields is in agreement with Holter and Johnson's nonlinear theory[21] of the helical instability in electron-ion plasmas.

These loops are easily and reproducibly obtained in p-type InSb at 77°K.

ACKNOWLEDGMENTS

The author is grateful to Dr. James E. Drummond for very helpful conversations and Robert W. Boice and Michael F. Berg for invaluable technical assistance.

[24] The author is grateful to H. P. Furth for suggesting this line of reasoning.